

ASPHALT MODIFIED BY PARTIALLY HYDROGENATED SBS TRI-BLOCK COPOLYMERS

M. A. VARGAS, A. E. CHÁVEZ, R. HERRERA*

FACULTAD DE QUÍMICA, UNAM, MÉXICO, D.F. 04510

O. MANERO

INSTITUTO DE INVESTIGACIONES EN MATERIALES, UNAM
MÉXICO, D.F. 04510. MEXICO

ABSTRACT

This work examines the modification of asphalt with hydrogenated poly (styrene-butadiene-styrene) copolymer containing different amounts of butadiene and ethylene-co-butylene. The polymer composition can be described generically as poly (styrene-[(butadiene)_{1-x}-(ethylene-co-butylene)_x]-styrene), where x is the hydrogenated fraction of the molecule. These hydrogenated (SBEBS) copolymers were produced by *in-situ* hydrogenation following a Ziegler-Natta catalytic reaction of poly (styrene-butadiene-styrene) tri-block copolymers (SBS), which were previously synthesized by anionic polymerization. Control over the hydrogenation time produces SBEBS polymers with various degrees of saturation of the polybutadiene block, as characterized by FTIR, ¹HNMR, differential scanning calorimetry (DSC) and gel permeation chromatography (GPC). Polymer-modified asphalts (PMA) were obtained by a high-temperature mixing process with AC-20 asphalt (Salamanca, Mexico) and SBS or SBEBS copolymers. PMA samples were characterized before and after high-temperature storage tests by fluorescence microscopy, rheometry, and mechanical tests. Results indicate that PMA obtained from SBEBS contain a polymer matrix with well-dispersed asphalt rich phase, with improved mechanical and thermal stability over those PMA produced with SBS. Compatibility between SBEBS and the aromatic fraction of maltenes can explain the dispersion of the polymer in asphalt and the enhanced properties.

INTRODUCTION

Asphalt mechanical properties and its thermo-oxidative resistance can be improved by blending the asphalt with copolymers. Block polymers, such as poly (styrene-butadiene) (SBR), poly (styrene-butadiene-styrene) (SBS), and poly (styrene-(ethylene-co-butylene)-styrene) (SEBS) are fairly compatible with asphalt. Polymer-modified asphalts (PMA) possess improved mechanical properties along a wide temperature range, as compared to those of neat asphalt.¹⁻⁸ Relatively small amounts of polymer (3 to 8 wt %) can improve the rheological properties of asphalt provided that compatibility exists between the modifier polymer and the asphalt.^{3,5,8}

Asphalt can be described as a mixture of oligomers (with molecular weights ranging from 500 to 3000) which can be separated and characterized by chromatography; four components can be identified: asphaltenes, aromatics, resins, and saturated compounds.^{3,5,8} In addition, two fractions can be extracted according to its n-heptane solubility: maltenes (soluble phase) and asphaltenes (insoluble fraction). Blends of asphalt and styrene-butadiene copolymers present a two-macrophase morphology: the first one is constituted by the polymer swollen by maltenes and the second one includes the asphaltenes and the rest of the maltene fraction which is not associated to the polymer.^{3,8-11} The polymer phase itself presents two microphases: the maltene-swollen polybutadiene phase and the polystyrene-rich domains, which serve as nodes of the polymer network.¹⁰⁻¹²

Di-block and tri-block copolymers (SBR and SBS, respectively) tend to degrade during both production and treatment of PMA, since they possess unsaturated bonds that are subjected to reactions of free-radical chemistry upon exposure to UV light, or during thermal and mechanical processes.^{2,13,14} Consequently, polymer chains may undergo crosslinking, chain scission and

* Corresponding author. Ph: (52)5622-5360; Fax: (52)5622-5355; email: rherrera@servidor.unam.mx.

grafting, resulting in either degradation of the PMA or stiffening of polymer macrophase, thus modifying the processability and adhesive properties of PMA.^{13,14} These effects are accentuated in regions experiencing extreme temperatures changes; therefore, production of highly resistant PMA requires polymers with enhanced thermal, mechanical, and chemical properties and furthermore, being compatible with asphalt.^{1,3,5,7,12} Thermal stability of polymer-modified asphalts is a function of the polymer degree of dispersion, which can be assessed by measuring the extent of macrophase separation when PMA is subjected to high-temperature storage tests.^{3,5,7,15}

Alternatively, chemical modification of unsaturated polymers, such as SBR and SBS, carried out by catalytic hydrogenation, offers a useful method to produce polymers with distinct properties.^{2,16-24} By a systematic reduction of the amount of double bonds, the physical properties of the polymer such as tensile strength, elongation, thermal and light stability, permeability to moisture, temperature-cycle damage resistance, and resistance to chemicals agents (ozone, fats, oils and solvents) may be improved.¹⁶⁻²⁴ Accordingly, due to the considerable advantages of SEBS copolymers, their blends with asphalt exhibit higher resistance to heat, permanent deformation, oxidation, and UV light.^{1-3,5,16} The improvement of asphalt mechanical properties with SEBS copolymers is associated to the presence of the ethylene-butylene block,^{17,18,24} which contains a certain amount of crystalline fraction and helps in road conditions presenting high loads or drastic temperature changes.^{1,5,8,12} However, high crystallinity does diminish polymer solubility with asphalt and processability.²

The polymers that are most compatible with asphalt are those with solubility parameters in the range of 7.6 to 8.6.²⁵ The solubility parameters for polybutadiene and ethylene-butylene (middle blocks of SBS and SEBS, respectively) in aromatic compounds are 8.4 and 7.9, respectively. According to these data, SEBS is to some extent more compatible with maltenes than SBS, and consequently, a better dispersion in the asphalt matrix may be expected.

In the current literature, analysis on asphalt modification with SBR, SBS, or SEBS are reported, but attention has not been given to asphalt modification with partially hydrogenated SBS, and this is the subject of the present work.

Polymer hydrogenation requires mild reaction conditions to avoid unwanted side reactions such as crosslinking and chain scission, which may cause a catastrophic loss of the sought polymer properties.^{16,18} Several catalytic methods for both homogeneous and heterogeneous hydrogenation have been developed for polydiene-containing polymers, namely SBS.¹⁶⁻²⁴ Homogeneous catalytic processes are preferred among others because of their superior selectivity.^{16,18,21} Wilkinson and Ziegler-Natta type catalysts exhibit high activity and selectivity under mild conditions, and therefore they can be used to selectively hydrogenate the isomers of the polybutadiene block (1,4-cis, 1,4-trans, and 1,2-vinyl).^{16,18,19}

This work analyzes the compatibility and performance of asphalt AC-20 (Salamanca, Mexico) modified with a series of partially hydrogenated SBS polymers, which were synthesized by varying the hydrogenation reaction times of the precursor polymer. Changes in the mechanical and rheological properties, apparent viscosity, morphology, thermal stability, and service temperature of the PMA produced from hydrogenated polymers are analyzed using as a reference the properties of PMA produced from the non-hydrogenated precursor (SBS).

EXPERIMENTAL

SAMPLE PREPARATION

Materials. — Nitrogen and ultrahigh purity (99.99%) hydrogen (supplied by Linde Co. Mexico) were used as received. Dynasol Elastomeros S.A. de C.V., former Industrias Negromex, Mexico, supplied the butadiene and styrene monomers, and cyclohexane (solvent). The solvent and monomers were passed through molecular sieves and alumina, and stored under nitrogen

atmosphere. Nickel (II) acetylacetonate (catalyst) with purity higher than 98%, and n-butyl lithium (cocatalyst) with 16% content in cyclohexane, were purchased from Merck, USA and FMC, USA, respectively. They were used as received.

AC-20 asphalt (PEMEX-Mexico) was used to prepare the PMA samples. The composition of the asphalt was 20 wt % asphaltene and 80 wt % maltene (solubility in n-heptane ASTM D3279-90). Asphalt physical properties were: penetration: 46 dmm (ASTM-D5, 25 °C); softening point: 56 °C (ASTM-D36); viscosity: 395 Pas (ASTM-D4402, 135 °C).

Poly (styrene-[(butadiene)_{1-x}-(ethylene-co-butylene)_x]-styrene) copolymers, referred herein as SBEBs, were produced by partial hydrogenation of poly (styrene-butadiene-styrene) polymers (SBS).^{16,18} The precursor SBS polymers were synthesized by sequential anionic polymerization of known amounts of styrene and butadiene using n-butyl lithium and cyclohexane as initiator and solvent, respectively. A series of partially saturated polymers were prepared by *in-situ* homogeneous catalytic hydrogenation of SBS using a nickel acetylacetonate/n-butyl lithium catalyst, maintaining a constant hydrogen pressure (semi-continuous process). Control of the reaction time allows the production of three SBEBs structures with various degrees of hydrogenation: 22, 52 and 77 %, (global hydrogenation was measured by ¹HNMR) identified herein as SBEBs-22, SBEBs-52, and SBEBs-77, respectively. Table I shows the reaction conditions for the production of SBS by anionic polymerization and the homogeneous catalytic hydrogenation of SBS. The microstructure details of the precursor polymer and partially hydrogenated moieties are presented in Table II.

TABLE I
REACTION CONDITIONS FOR THE (a) PRODUCTION OF
SBS BY ANIONIC POLYMERIZATION AND (b) CATALYTIC HYDROGENATION OF SBS

(a) Anionic polymerization	
Monomers	1,3-Butadiene; Styrene
Solvent	Cyclohexane
Initiator	n-butyl lithium
Temperature	75 °C
Pressure	534 kPa
(b) Catalytic hydrogenation	
Solvent	Cyclohexane
Catalyst	Nickel acetylacetonate/n-butyl lithium
Temperature	50 °C
Pressure	445 kPa
Polymer	Hydrogenation time (min)
SBEBs-22	30
SBEBs-52	60
SBEBs-77	120

TABLE II
MICROSTRUCTURE OF THE PRECURSOR POLYMER SBS, AND PARTIALLY HYDROGENATED POLYMERS BY FTIR AND ¹HNMR

Polymer	Styrene	Vinyl	Trans	Vinyl	Trans	Partially	Vinyl	Trans/cis	Vinyl	Trans/cis	Global
	(%)	(%)	(%)	hyd. (%)	hyd. (%)	hyd. (%)	(%)	(%)	hyd. (%)	hyd.	hyd.
		FTIR	FTIR	FTIR	FTIR	FTIR	¹ HNMR	¹ HNMR	¹ HNMR	(%) ¹ HNMR	(%) ¹ HNMR
SBS	30	10	45	0	0	0	9.0	91	0	0	0
SBEBS-22	30	8.5	40	15	12	12	6.0	72	33	21	22
SBEBS-52	30	4.6	34	54	24	30	0	48	100	47	52
SBEBS-77	30	0	21	100	53	62	0	23	100	75	77

Samples of polymer-modified asphalt (PMA) were produced by a high-temperature mixing process using AC-20 asphalt and either SBS or SBEBS. 200 g of asphalt were heated to 180 °C in a small tank with stirrer, and then a given amount of polymer (8 wt %) was gradually added under continuous stirring (500 rpm); the mixture was further stirred for 4 hours to ensure incorporation of polymer into the asphalt matrix. During the entire process, the vessel was maintained under a dry nitrogen atmosphere to minimize polymer degradation.

CHARACTERIZATION

Infrared spectroscopy was carried out in a Perkin-Elmer 1605 FT-IR spectrometer, equipped with a KBr cell for polymer/CCl₄ solutions analysis (0.0115 g/ml). Spectra were acquired within the 1000–600 cm⁻¹ range, and signals at 910 cm⁻¹ and 967 cm⁻¹ were used to determine the amount of 1,2-vinyl and 1,4-trans butadiene isomers, respectively. The constant styrene signal located at 699 cm⁻¹ was used as internal standard. Hydrogenation percentages of 1,2-vinyl and 1,4-cis isomers of SBEBS were calculated with respect to the reference composition of the precursor SBS.^{16,18,19,21}

A Varian Unity Inova 300 MHz spectrometer provided the ¹HNMR spectra. Deuterated chloroform solutions containing approximately 5 wt % polymer were analyzed using tetramethylsilane as internal standard. The degree of hydrogenation was estimated from the peaks area of the olefinic proton signals at 4.6 ppm (1,2-vinyl) and 5.8 ppm (1,4-cis and 1,4-trans) of both SBEBS and SBS.

Gel permeation chromatography (GPC) was performed on a HP 1090 liquid chromatograph, equipped with gel columns (10⁵ and 10⁴ Å) maintained at 35 °C using THF as carrier (1.0 ml/min). Tetrahydrofuran solutions of the polymer and standard polystyrene (0.012 g/ml) were analyzed.

X-ray diffraction patterns of the polymer (SBS) and hydrogenated polymers (SBEBS) were provided by a Siemens D 5000, KαCu at λ = 1.5406 Å, with an angle range from 2° to 45° (2 θ).

Thermal analysis of polymer and asphalt samples was carried out in a Dupont-910 differential scanning calorimeter operated within a temperature range of -130 °C to 130 °C, applying a heating rate of 10 °C/min under nitrogen atmosphere. Neat and modified asphalts were analyzed after 24 hours of thermal equilibration. All thermograms were recorded after two heating/cooling cycles and results from the second cycle are reported.

Polymer macro-phase distribution for PMA samples was observed through a Carl-Zeiss KS 300 fluorescence microscope. PMA samples were examined at room temperature using an excitation wavelength in the range of 390 to 450 nm and 20X magnification. The polymer phase appeared white and the asphalt-rich phase was dark. An image analyzer program was used to estimate polymer volume fraction.

Apparent viscosity of neat asphalt and PMA samples was determined using a Brookfield rotational viscometer (Model DV-III+) at various temperatures: 135, 150, 160 and 180 °C with a

rotating speed of 60 rpm.

Linear viscoelastic properties of asphalt and the PMA systems were measured in a strain-controlled rheometer AR-1000N using the parallel plate fixture (1 mm gap and 25 mm diameter). Frequency sweeps were applied from 0.1 to 100 rad/s at a strain amplitude within the linear viscoelastic range for a given temperature (-5, 15, 25, 40, 60, 75 and 100 °C). Temperature sweeps (-5 to 120 °C with 2 °C/min increments) were performed at a fixed frequency (1 rad/s). Upon heating the sample to its softening point, the top plate was brought into contact with the sample. Thermal equilibration of 15 minutes prior to isothermal tests was allowed.

Storage stability of PMA samples was determined according to the AASHTO procedure.^{3,5,15,26} 100 g of sample was placed into a glass tube (35 mm diameter and 190 mm height) internally wrapped with aluminum foil, and stored vertically in an oven at 180 °C for 72 hours. The sample was then cooled to room temperature and cut transversally into three equal sections. Top and bottom sections were characterized by the ring-and-ball softening method, rheometry and fluorescence microscopy.

RESULTS AND DISCUSSION

PARTIALLY HYDROGENATED SBS COPOLYMERS

The saturation degree of polybutadiene isomers was calculated from both infrared and nuclear magnetic resonance data. FTIR spectra of partially hydrogenated copolymers indicate that the spectrum of the intensity for 1,2-vinyl and 1,4-trans isomers (910 and 960 cm^{-1} , respectively) decreased with increasing level of hydrogenation, as shown in Figure 1. In addition, no observable change in the signal characteristic of styrene blocks (699 cm^{-1}) was detected after hydrogenation and therefore, it can be used as reference. In the case of the copolymer with the highest degree of hydrogenation (SBEBS-77), the vinyl band disappeared completely, indicating complete saturation of 1,2-vinyl isomer and furthermore, it shows that the remaining polybutadiene contains 1,4-cis and 1,4-trans unsaturations only, as previously reported¹⁶. FTIR analysis provided the degree of hydrogenation of the SBEBS copolymers based on the relative amounts of 1,2-vinyl and 1,4-trans isomers, with the non-hydrogenated SBS serving as reference.^{16,19,21}

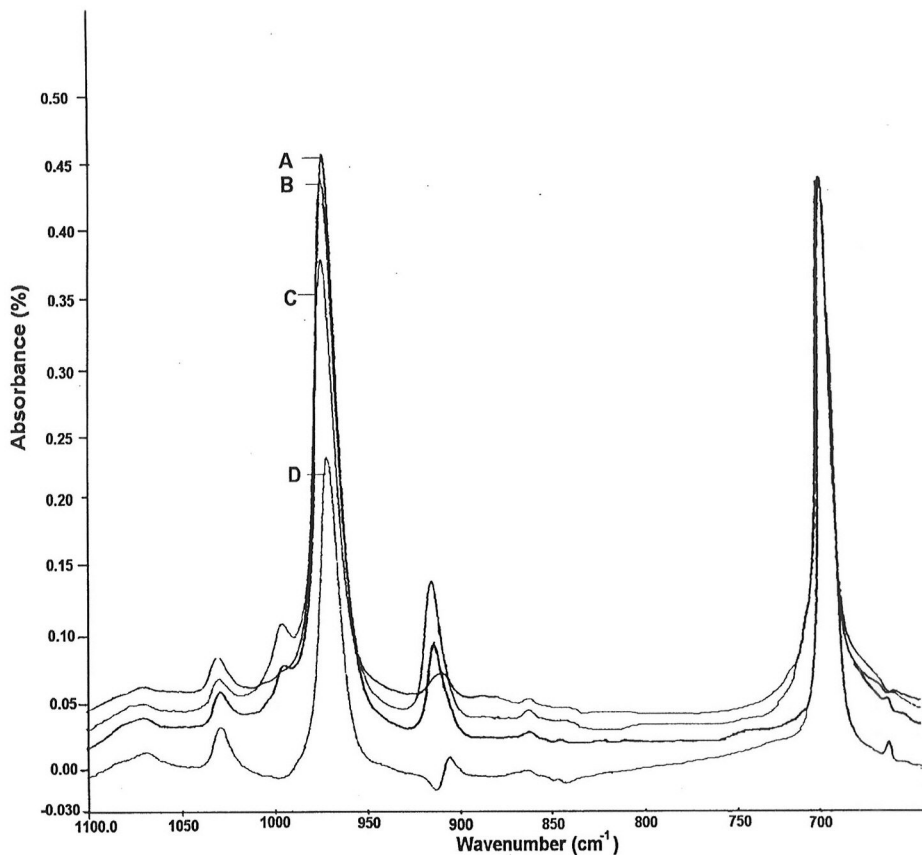


FIG. 1.— FTIR spectra of the (A) precursor polymer SBS; and hydrogenated polymers (B) SBEBS-22; (C) SBEBS-52; and (D) SBEBS-77.

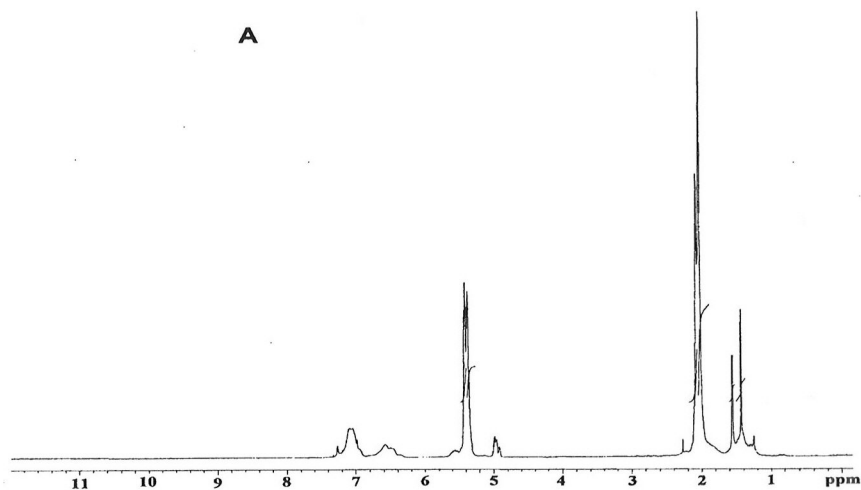


FIG. 2.— ¹H-NMR spectra of the precursor polymer (A) SBS; and hydrogenated polymer (B) SBEBS-77.

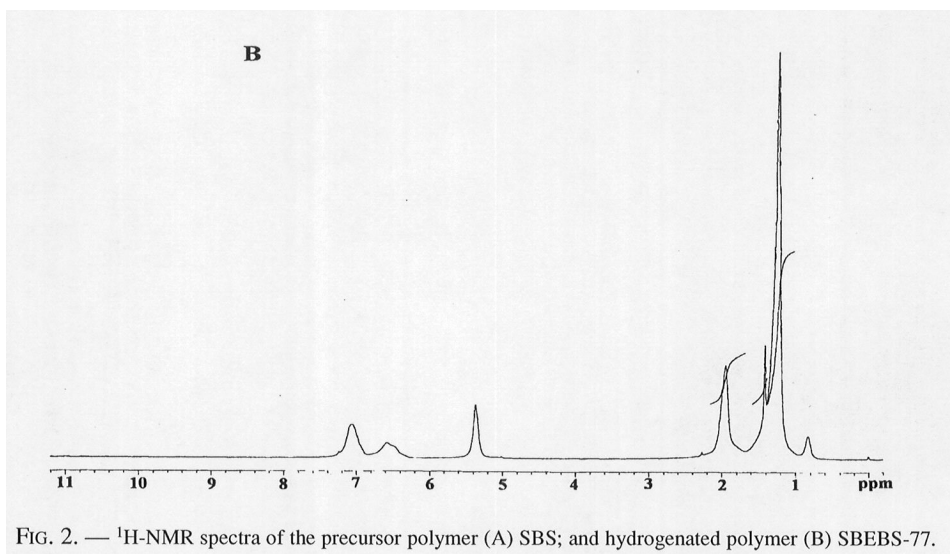


FIG. 2. — $^1\text{H-NMR}$ spectra of the precursor polymer (A) SBS; and hydrogenated polymer (B) SBEBBS-77.

Figure 2 shows the $^1\text{H-NMR}$ spectra of precursor and partially hydrogenated polymers. Saturation of the polybutadiene double-bonds is confirmed by the decrease or absence of olefinic proton signals at 4.6 ppm (1,2-vinyl) and 5.8 ppm (1,4-cis and 1,4-trans). The degree of hydrogenation was estimated by measuring the decrease in the peak areas corresponding to the three SBEBBS isomers and the precursor polymer SBS. Table II shows the results of FTIR and $^1\text{H-NMR}$ analysis in terms of the percentage of the isomers and the degree of hydrogenation determined by either technique. Results obtained from both methods indicate that the amount of polybutadiene isomers decreased as the hydrogenation time increased, and furthermore, they show a higher reactivity, with 1,2-vinyl bonds, in agreement with previous reports.^{16,24} Lower degrees of saturation were estimated from the FTIR analysis as compared to $^1\text{H-NMR}$ since, for the former, the degree of saturation was calculated in terms of the 1,2-vinyl and 1,4-trans isomers, and for the latter, contribution from the 1,4-cis is additionally considered. In general, results suggest that the four polymers considered in this study differ only in the chemical composition of their middle-blocks, while the composition of their end-blocks remains the same.¹⁶ These results indicate that the procedure followed allows to produce copolymers with different chemical and physical properties to those of the precursor polymer, as it is shown in Table III.

TABLE III
POLYMER PROPERTIES

Polymer	Mn, g/mol	Mw, g/mol	D	Tg, °C	ΔHm , J/g	Tm, °C	Crystallinity by DSC, %	Crystallinity by X-ray diffract., %
SBS	123 000	132 000	1.07	-91	-	-	Amorphous	Amorphous
SBEBBS-22	125 000	134 000	1.07	-86	-	-	Amorphous	Amorphous
SBEBBS-52	128 000	137 000	1.07	-78	8.0	30.34	4.0	4.8
SBEBBS-77	128 000	131 000	1.02	-59	12.0	43.71	6.1	7.0

Chromatograms for the parent polymer and partially hydrogenated polymers are presented in Figure 3 and results from the GPC analysis are shown in Table III. Results indicate similar molecular weights, and no significant changes in the polymers molecular weight distribution occurred as a result of the hydrogenation process. Therefore, the hydrogenation conditions were adequate to favor saturation of polybutadiene isomers over other possible reactions like poly-

styrene saturation, chain scission, or crosslinking. Glass transition temperature (T_g), melting enthalpy (ΔH_m), melting temperature (T_m) and crystallinity (%) of SBS and SBEBS are also shown in Table III.

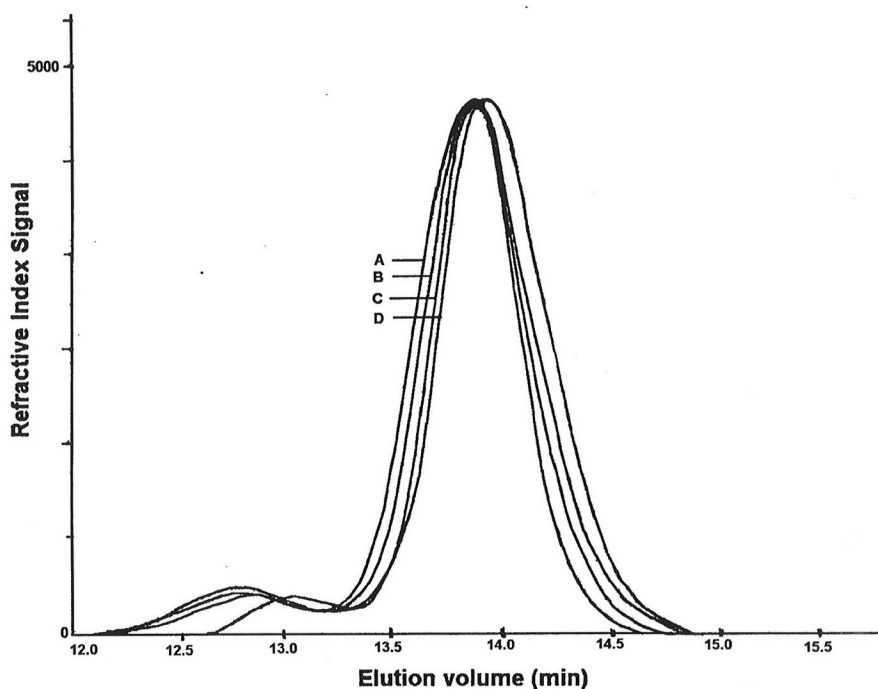


FIG. 3. — GPC traces of the precursor polymer (A) SBS; and hydrogenated polymers (B) SBEBS-22; (C) SBEBS-52; and (D) SBEBS-77.

Results from the thermal analysis of the parent and hydrogenated copolymers are disclosed in Figure 4 and in Table III. In Figure 4, except for the SBEBS-77 which is the more hydrogenated sample, with the smallest amount of polybutadiene, each polymer presents a clear glass transition temperature (T_g) corresponding to the elastomeric block, which increases with the amount of polymer hydrogenation. In addition, SBEBS-52 and SBEBS-77 present an endothermic peak associated with the crystalline fraction. Saturation of the double bonds of polybutadiene isomers to render ethylene-co-butylene groups increases the molecular order (decrease in entropy). The degree of crystallinity was estimated from this endothermic signal using the heat of fusion of polyethylene (198 J/g) as a reference.^{16,17} These values are disclosed in the same table. Glass transition temperature (T_g) of the styrene group is located ca. 92° C for SBS and SBEBS-22, while for SBEBS-52 and SBEBS-77 determination of the T_g was difficult as the endothermic peak of those samples is broad.

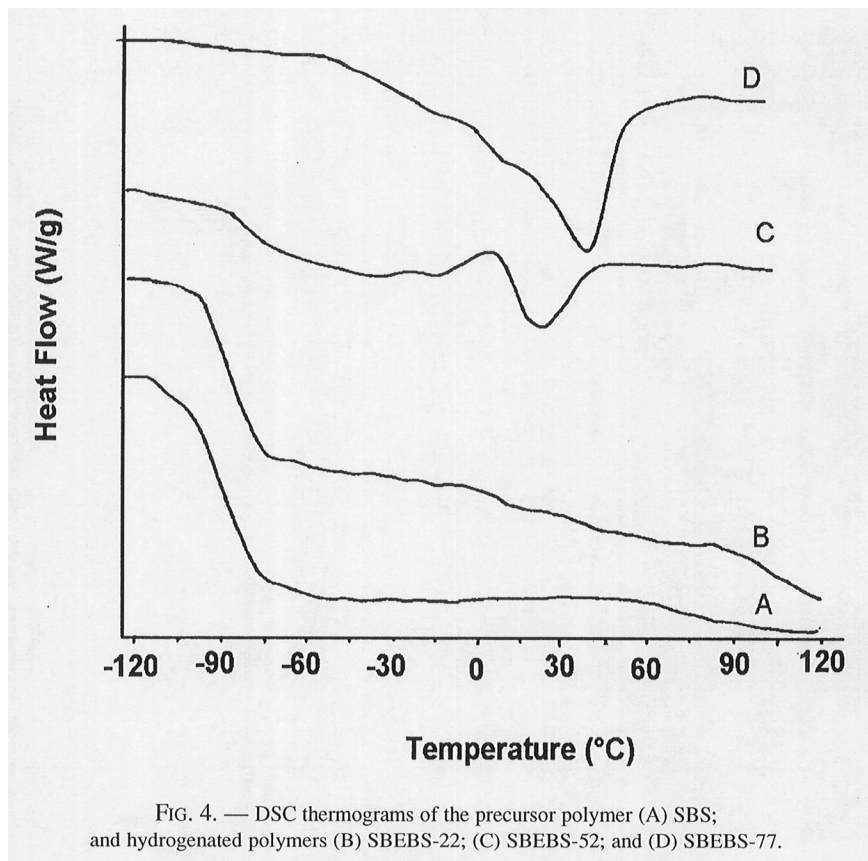


Figure 5 shows the X-Ray spectra for (A) SBS and (B) SBEBS-77. The hydrogenated polymer presents an evident crystalline fraction as revealed from comparison of the peak widths of the SBEBS-77 and the amorphous SBS. Percentage of crystallinity was estimated from the peak areas of the partially-crystalline SBEBS-52 and SBEBS-77 samples and that of the amorphous SBS according to the following Equation:¹⁷

$$\%crystallinity = \frac{A_{crystalline}}{A_{amorphous}} * 100 \quad (1)$$

Table III shows that results of the crystallinity fraction obtained with X-Rays agree with those of the DSC test.

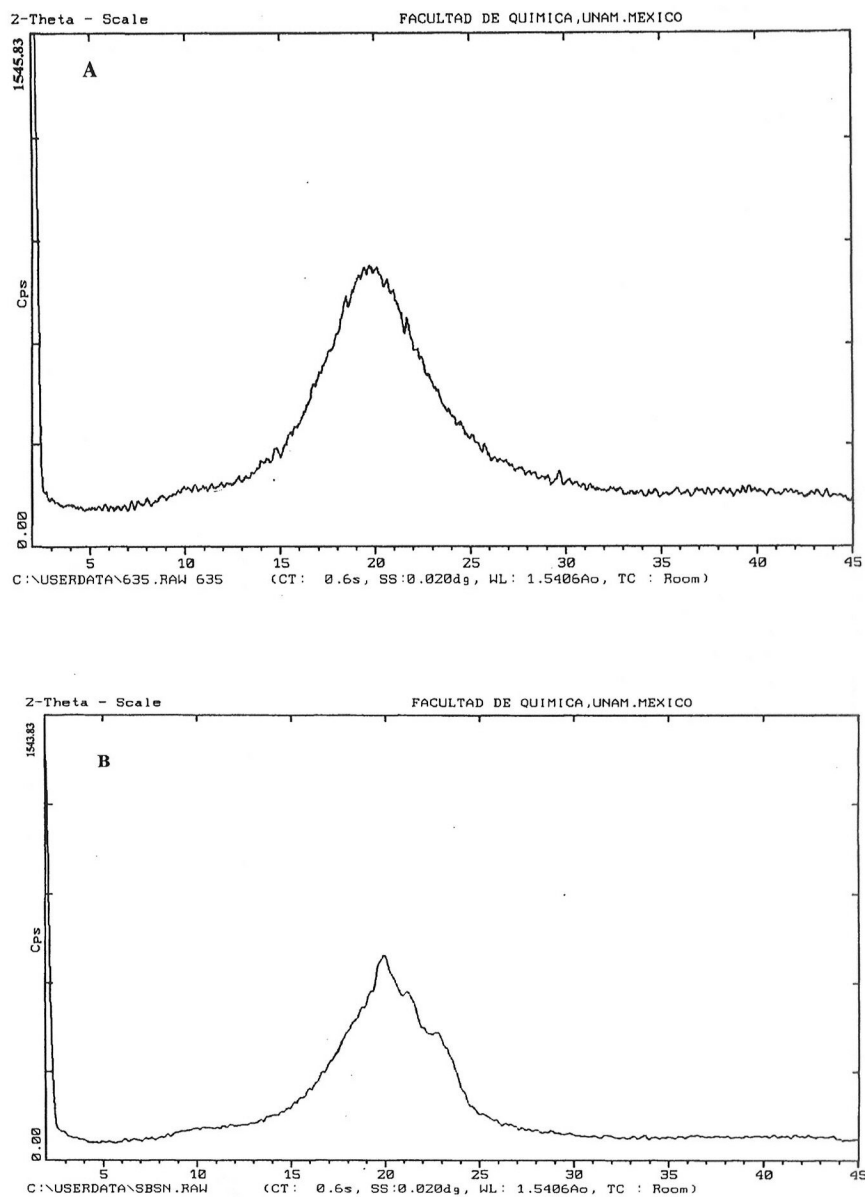


Fig. 5. — X-ray diffraction spectra of the parent polymer (A) SBS and hydrogenated polymer (B) SBEBS-77.

POLYMER-MODIFIED ASPHALT

MORPHOLOGY

Fluorescence microscopy images of PMA shown in Figures 6A-6D (PMA-0, PMA-22, PMA-52, and PMA-77) correspond to asphalts modified by SBS, SBEBS-22, SBEBS-52, SBEBS-77, respectively. Samples exhibit polymer (light field) and asphaltene (black field) macrophases, the former are identified with polymer swollen by asphalt aromatic compounds whereas the latter reveals asphaltene domains surrounded by resins, saturated and remaining aromatic compounds.^{3,5,9,10} These images also provide evidence of the degree of hydrogenation on

the morphology of PMA, since both the size and shape of the polymer macrophase are affected by polymer saturation. PMA-0 (produced from the non-hydrogenated polymer SBS) exhibited a "salami-type" polymer macro-phase of large particles (1.3 μm) with asphaltene inclusions, embedded in the asphalt matrix; these salami particles are dispersed in the asphalt matrix, which may also contain very small polymer particles (0.2 μm) Figure 6A. A completely different morphology to PMA-0 was displayed by PMA-22, where the polymer macrophase constituted the matrix, and the inclusions were large isolated salami-type particles of asphaltene (0.35 μm) Figure 6B. PMA-52 displayed better polymer distribution than PMA-0 and PMA-22. The polymer macrophase matrix shows only small asphalt inclusions (0.2 μm) Figure 6C. In contrast, the PMA-77 (which includes the polymer with the highest degree of hydrogenation, SBEBS-77), exhibited distinct morphology, different to the other PMA, Figure 6D. In this case the polymer macrophase matrix was present as a thin polymer lattice containing large asphalt particles (1.1 μm) with small polymer particles. We remark that the PMA investigated were prepared from polymers that differ only in the composition of their elastomeric middle block, using the same amount of polymer, both in weight percentage (8 wt %) and in number of polymer chains (since all polymers have practically the same average molecular weight and molecular weight distribution, Table III) and underwent similar mixing conditions. Therefore, the differences observed among these systems can only be attributed to the compatibility degree between the polymer and the asphalt. For example, by comparison of the morphology features of PMA-0 with those of PMA-52, it is apparent that SBEBS-52 was better incorporated into the asphalt matrix (Figures 6A and 6C). Consequently, the compatibility degree of the asphalt with SBEBS-52 was higher than that of asphalt with SBS, since the solubility parameters of the aromatic compounds are closer to those of SBEBS. However, the strikingly distinct morphology exhibited by PMA-77 (prepared from SBEBS-77, which has the highest degree of hydrogenation and highest crystallinity) is due to the fact that polymers with high crystallinity are generally not compatible with asphalt.²⁵ Therefore, the unique morphology and distribution of the polymer in PMA-77 result from a combination of two effects: solubility parameter value and crystalline content.

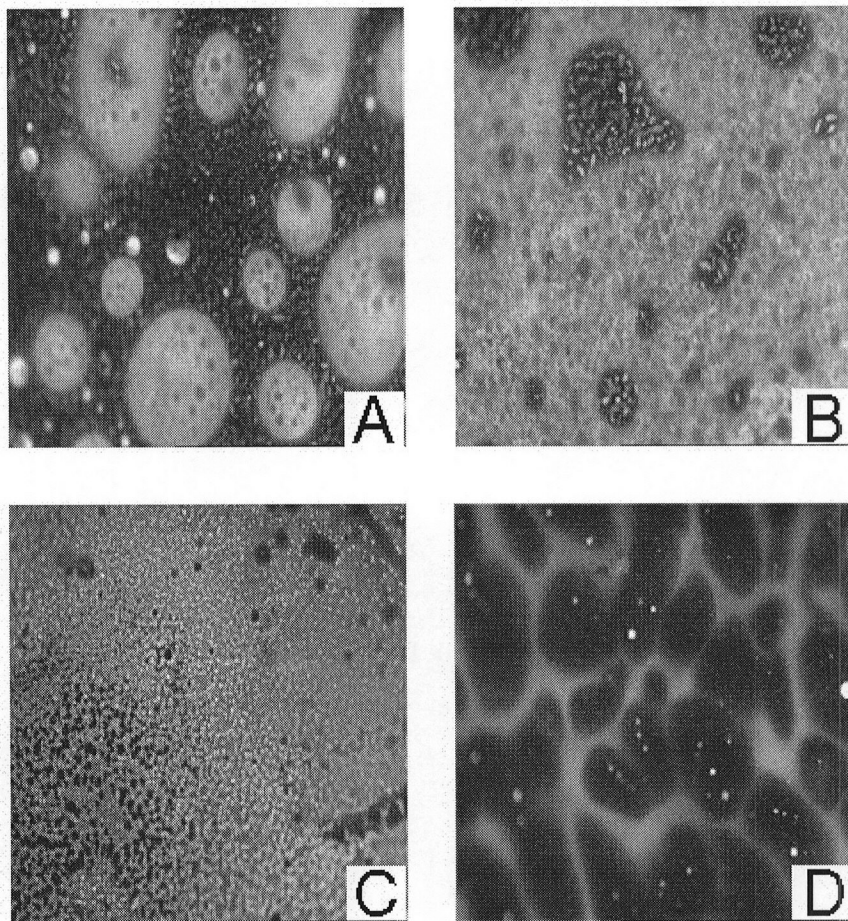


FIG. 6. — Morphology of blends: (A) PMA-0; (B) PMA-22; (C) PMA-52; and (D) PMA-77. Polymer content is 8 wt %. 20 X magnification.

THERMAL ANALYSIS

Thermograms for neat asphalt, and polymer-modified asphalt blends are presented in Figure 7. A complex thermal behavior is observed, reflecting the multi-component structure of these materials. Asphalt (Figure 7A) presents two T_g , one at -45°C , corresponding to the saturated fraction of asphalt, while the other T_g is associated to the aromatic fraction (around -10°C). In this case, T_g of resins (20°C) and asphaltenes (70°C) are not clearly discernible,^{6,8,27-29} due to a small asphaltene fraction (~ 20 wt %). In all PMA (Figures 7B-7E) two T_g are observed, one associated to the maltenes polymer swollen macrophase, increasing from -40 to -20°C , and the other one related to the asphaltenes-rich macrophase ($\sim 15^\circ\text{C}$). Furthermore, sample PMA-77 (Figure 7E) clearly depicts a wide endothermic peak (~ 10 - 50°C) associated to the crystalline fraction of the polymer (ethylene-butylene domains).⁸ This behavior reflects a lower compatibility among asphalt and the semi-crystalline polymer phase, as observed in the morphological features in Figure 7D. For this reason, in polymers with hydrogenation degree larger than 77%, compatibility with asphalt diminishes as phase separation becomes increasingly evident. Processing of these materials becomes increasingly difficult as well.

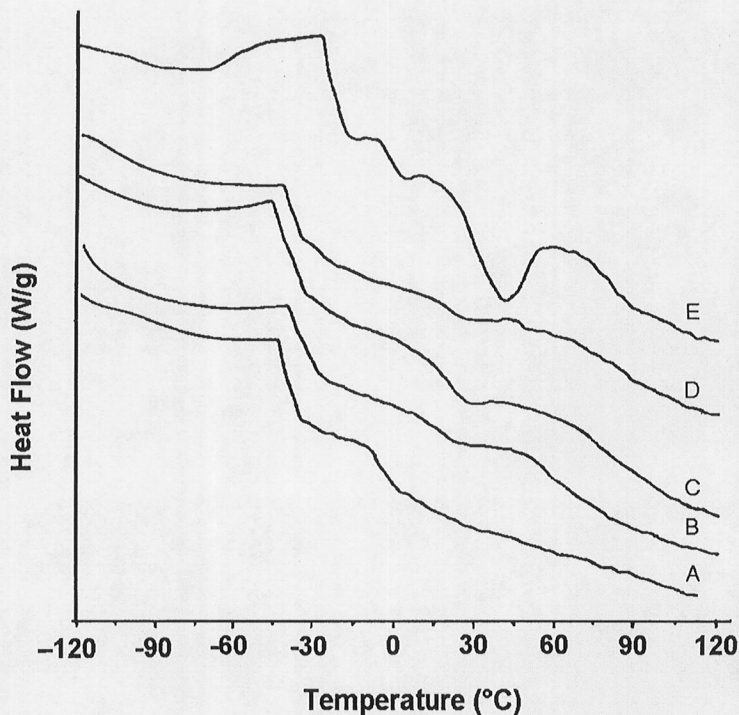


FIG. 7. — DSC thermograms of (A) asphalt AC-20, and blends: (B) PMA(0); (C) PMA-22; (D) PMA-52; (E) PMA-77.

APPARENT VISCOSITY

Figure 8 shows the apparent (Brookfield) viscosity of neat asphalt and that of the PMA measured at 180 °C. A significantly larger viscosity of PMA as compared to that of the unmodified asphalt is measured, increasing with the degree of hydrogenation for low extents. This increase levels off at high hydrogenation degrees, as viscosities of PMA-52 and PMA-77 are similar. The viscosity-temperature behavior of polymer-modified asphalt samples is shown in Figure 9 as an Arrhenius plot, from which the activation energy for each PMA was calculated⁷ and presented in Table IV. An increase in the activation energy with the degree of hydrogenation of the polymer is observed, ascribed to the presence of crystalline ethylene-butylene segments and to the asphalt distribution within the polymer matrix.

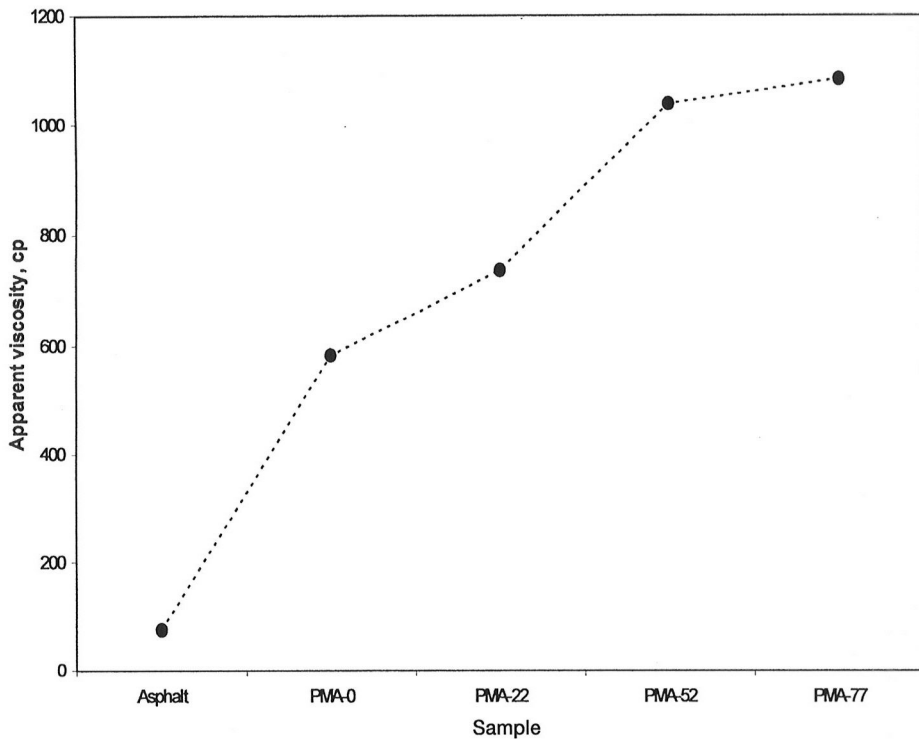


FIG. 8. — Effect of the hydrogenation of polymer on the viscosity of PMA at 180 °C with a shear rate of $\dot{\gamma} = \text{sec}^{-1}$.

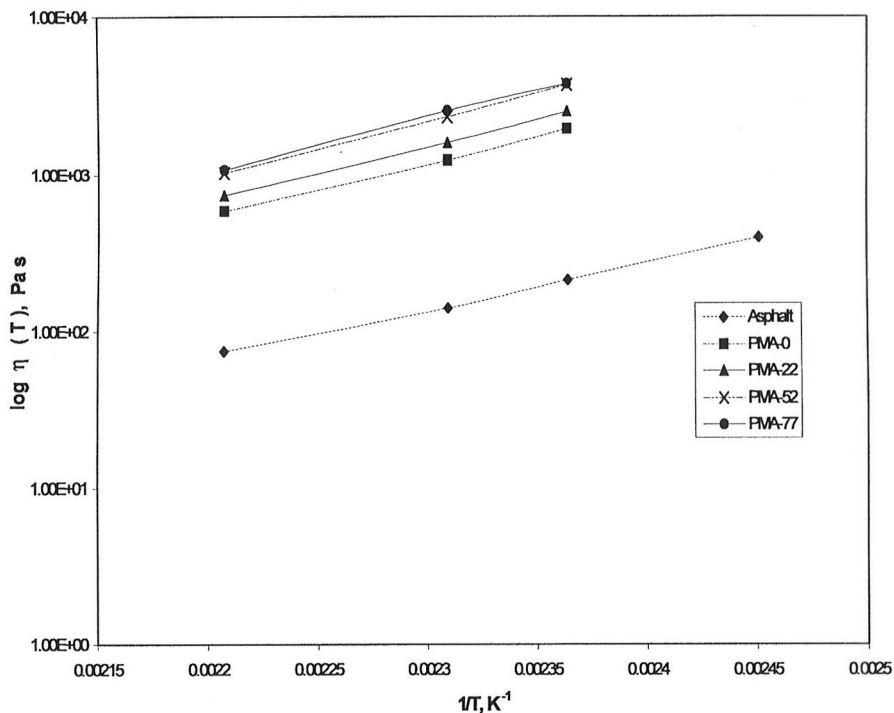


FIG. 9. — Arrhenius plot of the apparent viscosity of asphalt and blends.

TABLE IV
ACTIVATION ENERGY OBTAINED FROM FIGURE 9

Sample	E_{η} , kcal/mol
Asphalt	55.0
PMA-0	65.0
PMA-22	66.0
PMA-52	68.5
PMA-77	68.0

THERMAL STABILITY

The thermal stability of PMA was evaluated by subjecting the samples to a high temperature storage treatment (180 °C for 72 hours)^{3,5,7,26} and subsequently analyzing both the top and bottom parts of the sample by fluorescence microscopy, softening temperature measurements, and separation index (I_s).^{5,7}

The storage stability test produces various morphologies, which were characterized by fluorescence microscopy, as shown in Figure 10 for the top and bottom sections of each blend. Results indicate that some samples have undergone phase separation since their bottom and top sections exhibit different amounts of both polymer and asphalt macrophases, with a polymer-rich macrophase concentrated at the top section. Moreover, the difference is more pronounced for PMA-0; the morphology for its top section is a continuous polymer macrophase, while that at the bottom reveals an asphalt macrophase. Evidently, PMA-0 is unstable at elevated temperatures and tends to phase-separate. A strikingly different behavior was observed for PMA-52, since both parts display high amounts of polymer, revealing better thermal stability. The phase separation extent for PMA-22 has intermediate values between those of PMA-0 and PMA-52, while PMA-77 maintains a high polymer content in both top and bottom sections, thus revealing morphological features similar to those of PMA-52 (Table V shows the softening temperatures for the PMA samples).

A PMA criterion of stability defines a stable system that which exhibits softening temperatures differing by only 2 °C between the top and bottom sections.^{3,7,15} It is evident that PMA-0 is unstable since the difference in softening temperatures exceeded 20 °C. On the other hand, PMA prepared from partially hydrogenated polymers display similar softening temperatures for both top and bottom, and consequently, appears to be stable for high temperature storage.

Based on these results, phase separation is diminished by increasing the degree of polymer hydrogenation. A possible explanation considers that incorporation of polymer in the asphalt depends on the compatibility between the polymer and the aromatic components of asphalt.^{8,25} Compatibility is therefore a necessary condition to improve the physical properties of asphalt and to avoid phase separation.^{3,5-7} For example, by comparison of the morphology features of PMA-0 with those of PMA-52, it is apparent that SBEBS-52 was better incorporated into the asphalt matrix, thus rendering a blend with improved thermal stability (PMA-52). Phase separation is more evident in PMA-0, as observed in Figure 10 and Table V.

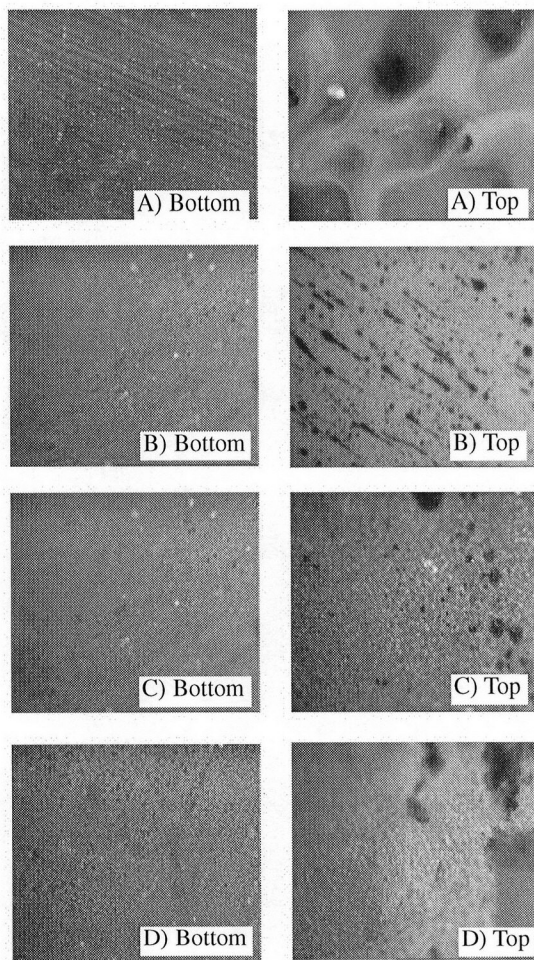


FIG. 10. — Morphology of the polymer/asphalt blends after storage stability tests: (A) PMA-0; (B) PMA-22; (C) PMA-52; and (D) PMA-77. 20 X magnification.

RHEOLOGICAL PROPERTIES

Complex modulus (G^*) and $\tan(\delta)$ of neat asphalt and PMA as a function of temperature at fixed frequency (1 rad/s) are shown in Figure 11. For neat asphalt, three regions of moduli behavior can be identified, namely, glassy, transition and terminal regions.⁵ SBEBS-modified asphalts exhibit a trend towards rubbery plateau region, slightly more evident than that of the SBS modified asphalt, manifesting a slight increase in the elasticity of the blend.

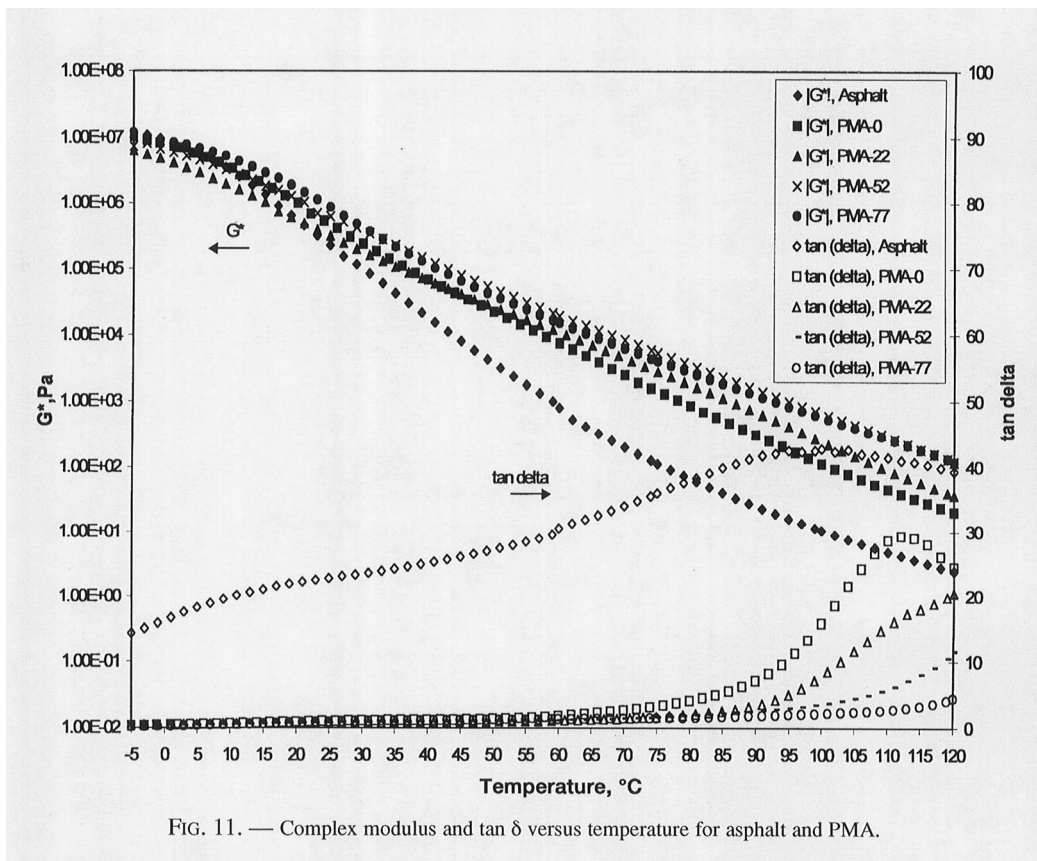


FIG. 11. — Complex modulus and $\tan \delta$ versus temperature for asphalt and PMA.

For high temperatures ($T > 50^\circ\text{C}$), polymer modification leads to an increase in the complex modulus and a decrease in the loss tangent, although the complex modulus approaches same value at high temperature for PMA-52 and PMA-77. It is also apparent that these two blends have practically the same modulus for all temperatures investigated. As the degree of hydrogenation increases, the PMA become more elastic at high temperatures, leading to superior resistance to permanent deformation.^{1,5,12} For temperatures lower than 40°C no substantial difference between the modulus for the PMA is observed, nonetheless PMA-0 and PMA-22 have the same modulus, which is smaller than that of PMA-52 and PMA-77. SBEBS modified asphalt samples do not present maxima in the loss tangent, in contrast to the maxima observed in the neat asphalt and PMA-0, indicating that the PMA produced from partially hydrogenated polymers are elastic throughout the temperature range examined.

The frequency-dependent storage modulus (G') at fixed temperature (75°C) for neat asphalt and blends is illustrated in Figure 12. It is clear that the PMA display higher elasticity than unmodified asphalt, and also that elasticity for the PMA increases with the degree hydrogenation of the parent polymer. The decreasing slope of the curves in the low frequency region is ascribed to rising level of entanglements and the formation of an elastic network. Such differences are larger at low frequencies (*i.e.* high temperatures).

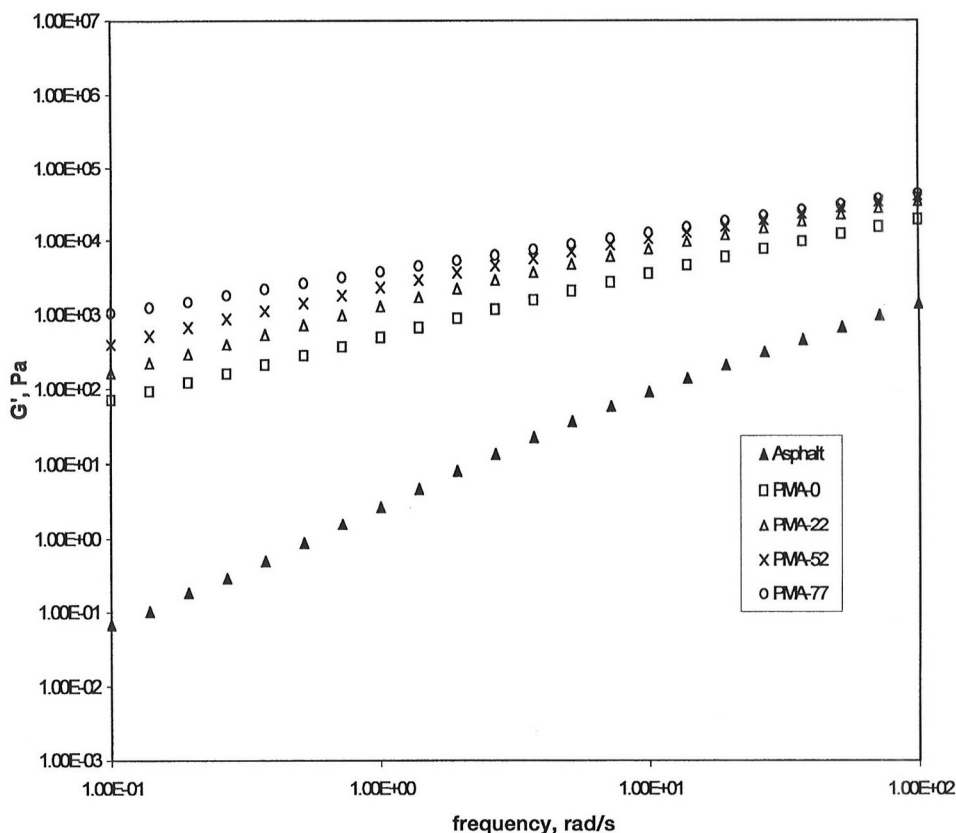


FIG. 12. — Elastic modulus versus frequency at 75 °C for asphalt and PMA.

Figure 13 shows the variation of the phase angle (δ) with complex modulus G^* ; these Black diagrams were generated from data taken at several frequencies and temperatures, and represent a sensitive test of the time-temperature superposition principle^{5,30,32} and the variations in the morphology or structure of the blends induced by thermo-mechanical stresses.³¹ As observed, a trend towards superposition of data is only seen at small phase angles ($\delta < 50$), *i.e.* at low temperatures, as the rheological behavior tends to that of an elastic solid.^{30,31}

Asphalts and blends differ in their rheological behavior.²⁸ Neat asphalt shows a continuous decrease of δ , whereas the polymer blends exhibit a very clear inflection point (or a minimum) at 80–35 ° ca. 1.5×10^1 – 1×10^5 Pa and a plateau of the complex modulus at ca. 1×10^3 – 1×10^6 Pa.

Reported data for asphalts suggest that they closely follow time-temperature superposition, which is not in the case for polymer-asphalt blends.^{30,31} However, as observed in Figure 13, superposition of asphalt and PMA data are only observed at low temperatures, which reflects the wide spectrum of relaxation times, also seen in the DSC data shown in Figure 7. Other works^{30,31} have suggested that superposition at elevated temperatures cannot be obtained due to high asphaltene and crystalline fractions contents. This is more crucial as the crystalline fraction content increases in the blends caused by hydrogenation of the polymer.

A larger plateau region is observed for the SBS-22 blend, while the SBS-77 blend displays a minimum. A phase angle minimum has been attributed to a hard/soft relaxation.⁶ Considering the morphology observed in Figures 6B and 6D, within the region of minimum phase angle, the polymer modulus dominates the blend modulus.

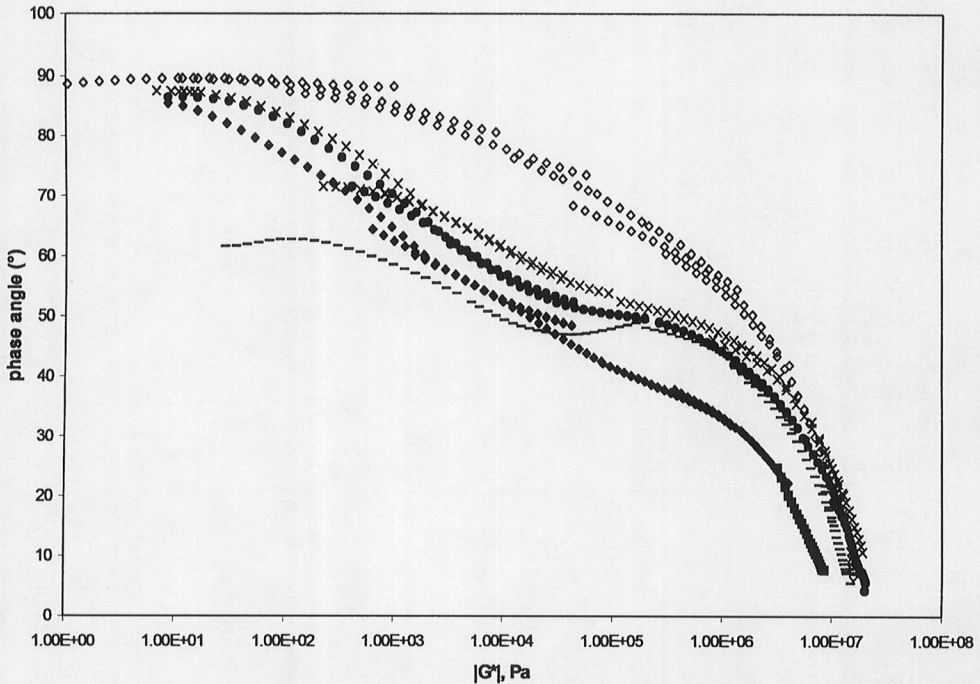


FIG. 13. — Complex modulus versus phase angle (black diagram) for (◇) asphalt; and (×) PMA-0; (●) PMA-22; (◆) PMA-52; and (—) PMA-77.

The Strategic Highway Research Program (SHRP)^{5,7,12} selected an empirical parameter, the *rutting factor*, to measure the rutting resistance contribution of an asphalt binder. The parameter is defined as the temperature at which $G^*/\sin \delta$ is equal to 1 kPa.

As seen in Table VI the magnitude of the *rutting factor* is dependent on the structure of the modifying polymer, in particular on the chemical composition of partially hydrogenated polymers, in agreement with other work.^{5,12} Table VI shows that the magnitude of the rutting factor is 59 °C for neat asphalt and increases from 78 °C to 95 °C for PMA-0 and PMA-77, respectively. PMA prepared with polymers having the largest degree of hydrogenation (PMA-52 and PMA-77) render similar values of the rutting factor.

TABLE V
STORAGE STABILITY OF POLYMER-MODIFIED ASPHALTS

Sample	Softening point, Bottom, °C	Softening point, Top, °C
PMA-0	78	98
PMA-22	84	84
PMA-52	81	81
PMA-77	80	81

TABLE VI
PERFORMANCE PARAMETERS

Sample	Temperature at which $G^*/\sin \delta = 1\text{kPa}$, °C
Asphalt	59
PMA-0	78
PMA-22	85
PMA-52	93
PMA-77	95

The thermal stability of PMA was also evaluated through the separation index, I_s , calculated from rheometric measurements at 25 °C and 10 rad/s as proposed in the SHRP:⁵

$$I_s = \frac{\log|G^*|_{Bottom}}{\log|G^*|_{Top}} \quad (2)$$

As illustrated in Figure 14, the degree of separation depends on the chemical structure of the polymer; PMA-52 appears to be the most stable and better dispersed sample, as shown by fluorescence microscopy results examined previously. Consequently, PMA-52 is the most thermally stable blend. These data clearly illustrate the effect of the chemical composition of the middle block on the high temperature properties of PMA produced from such hydrogenated polymers.

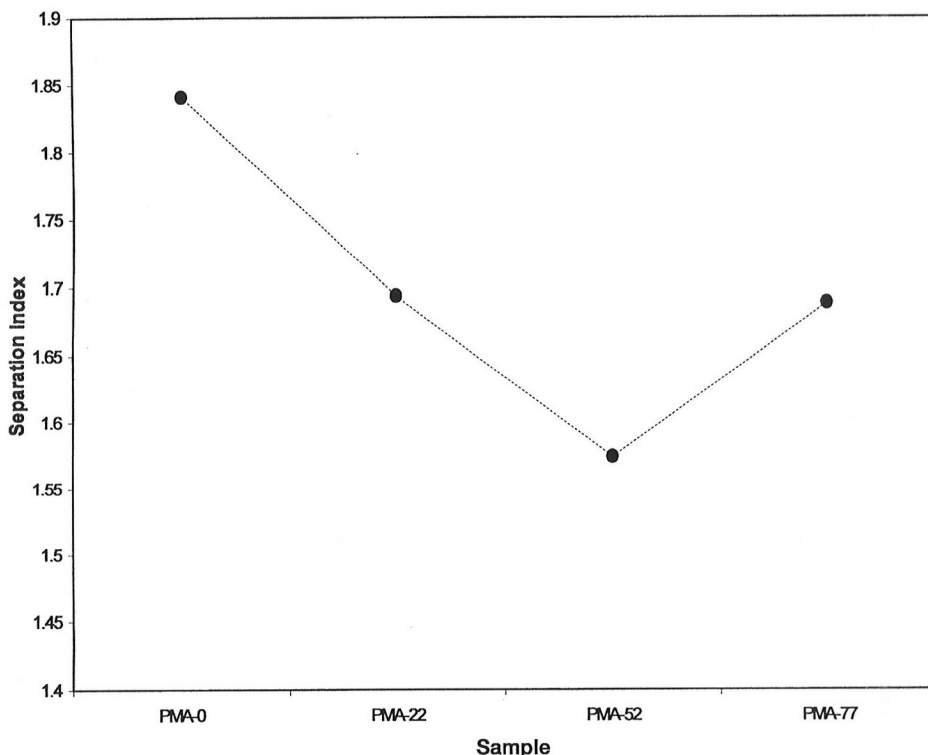


FIG. 14. — Separation index of PMA. Frequency is 10s^{-1} at 25 °C.

DISCUSSION AND CONCLUDING REMARKS

In this work, a detailed analysis of the effect of partial hydrogenation of SBS on the material properties of polymer-modified asphalt blends is presented. This analysis explores different degrees of saturation of the polybutadiene block of linear SBS, an aspect that has not been analyzed before. The concluding remarks are as follows:

- 1) Characterization of these polymers by means of GPC, FTIR, and ^1H NMR, established that hydrogenation conditions were adequate to favor saturation of the polybutadiene isomers over other reactions like chain scission, cross-linking or saturation of the polystyrene groups. Consequently, these polymers differed exclusively in the chemical composition of their elastomeric block, containing polystyrene blocks of the same molecular weight. Increasing the level of hydrogenation, enhanced transition temperatures and crystalline contents are obtained. Such increases are attributed to larger fractions of the ethylene-butylene units,^{8,16,17} as DSC and X-ray diffraction characterizations show.
- 2) Fluorescence micrographs show that the elastomeric block composition has an important effect on the morphology of PMA, since both the size and shape of the polymer macrophase depend on the degree of saturation of the polymer. The blend produced from the non-hydrogenated polymer exhibits a "salami-type" polymer macrophase of large particles embedded in the asphalt matrix, while blends produced from partially hydrogenated polymers display better polymer dispersion. Moreover, using the same amount of polymer (8 wt %), PMA with hydrogenated polymers undergo phase inversion, in contrast to PMA-0. Blends PMA-25 and PMA-50 having fine dispersion of the asphalt in the polymer matrix can be considered homogeneous systems. When the amount of polymer is large enough, 8 wt % in this series, the morphology of a continuous polymer macrophase with dispersed asphaltene macrophases is formed and the system exhibits substantial elastic response^{5,12} (see Figures 6B-6D).
- 3) DSC results indicate that the neat asphalt sample exhibits two glass transition temperatures, one around $-45\text{ }^\circ\text{C}$, attributed to the present of saturates, and another one, due to resins ($-10\text{ }^\circ\text{C}$). On the other hand, PMA also exhibit two Tg, one attributed to the polymer-rich macrophase, increasing from -40 to $-20\text{ }^\circ\text{C}$, and the other one related to the asphaltene-rich macrophase at ca. $15\text{ }^\circ\text{C}$ (Figures 7B-7E). PMA-77 clearly depicts a wide endothermic peak ($\sim 10\text{-}50\text{ }^\circ\text{C}$) associated to the crystalline fraction of the polymer ethylene-butylene domains (Figure 7E), which induces lower compatibility with asphalt.
- 4) Fluorescence microscopy observations reveal that some samples undergo phase separation (PMA-0) since their bottom and top sections exhibit different amounts of polymer and asphalt macrophases. PMA-52 showed the highest thermal stability. In contrast, the stability of SBS-modified asphalt at high temperatures is relatively low. An explanation is offered in terms of the solubility parameter of the polymer in aromatic compounds.
- 5) PMA exhibit significantly higher viscosity than that of neat asphalt, increasing with the degree of hydrogenation, but this increase levels off at large hydrogenation extents as similar viscosities are measured in PMA-52 and PMA-77. The activation energy for each PMA, as calculated from an Arrhenius-type model, is proportional to the degree of hydrogenation of the polymer.
- 6) PMA having a continuous polymer macrophase present high elasticity, in contrast to those systems with small polymer domains dispersed in the asphalt that tend to behave as neat asphalt. Results indicate that PMA made from partially hydrogenated (SBEBS) are more elastic than those produced from SBS, since SBEBS are better dispersed in the asphalt matrix.
- 7) The high-temperature stability of the PMA can be assessed from the variation of the complex modulus, G^* , and loss tangent, $\tan(\delta)$, as functions of temperature in the range

of interest. Particularly, increasing polymer hydrogenation leads to a slight plateau region for $\tan(\delta)$ and large values of G^* . Data reveal increased elasticity resulting from increased polymer-asphalt molecular interactions. PMA-52 and PMA-77 exhibit better mechanical properties, despite their different morphologies. The fact that the properties of PMA-77 did not show substantial improvements over those of PMA-52 may be attributed to the crystalline character of the highly hydrogenated polymer affecting polymer/asphalt compatibility. Samples of SBEBS-modified asphalt do not present maxima in the loss tangent as observed in the neat asphalt and PMA-0, indicating that such PMA is elastic throughout the temperature range. The higher elasticity measured in the SBEBS-modified asphalts over that measured in the SBS-modified asphalt and neat asphalt (as proved by the behavior of the elastic modulus, G' , in a frequency range of 10^{-1} to 10^2 rad/s at 75°C , Figure 12) suggests the presence of entanglements that lead to the formation of an elastic network.

- 8) Neat asphalt and PMA samples are complex thermo-rheological systems, as shown by their Black diagrams. The lack of time-temperature superposition is attributed to the multi-phase structure of these systems. Nevertheless, data clearly indicate that the rheological behavior of asphalt and blends is different, since neat asphalt exhibits a large magnitude and a continuous decrease of the phase angle within the entire range of complex modulus (G^*), whereas the polymer blends exhibit an inflection point and a plateau in G^* , revealing that the linear viscoelastic properties of the polymers increase with the polymer degree of hydrogenation.
- 9) This study reveals that the magnitude of the *rutting factor* ($G^*/\sin\delta$) depends on the composition of partly hydrogenated polymer-modifier; the polymers with large degree of hydrogenation are more resistant to rutting.

In conclusion, these results demonstrate improvements obtained in the high temperature properties of PMA. In particular, it has been shown that an increase in the degree of hydrogenation of the SBS tri-block copolymers favors polymer dispersion in the asphalt matrix, increasing the temperature resistance and stability of PMA.

ACKNOWLEDGEMENTS

The authors gratefully acknowledge the facilities provided by the Polymer and Chemical Engineering Laboratories and the Materials Research Institute at UNAM (National University of Mexico). Raw materials from Dynasol Elastómeros de México, and funds from DGEP project IN-114303, and CONACYT project G-27837-U are also acknowledged.

NOMENCLATURE

$ G^* $	Complex modulus	Pa
G'	Storage modulus	Pa
G''	Loss modulus	Pa
I_s	Separation index	
$ G^* _{\text{Bottom}}$	Complex modulus bottom section	Pa
$ G^* _{\text{Top}}$	Complex modulus top section	Pa
E_η	Activation energy	kJ/mol
R	Universal gas constant	J/molK
η	Apparent viscosity	Pa s
δ	Phase angle	
$\tan\delta$	G''/G'	
SBS	Styrene-butadiene-styrene block copolymer	

SEBS	Styrene-ethylene-butylene-styrene block copolymer
SBEBBS-22	Poly (styrene-(butadiene-ethylene-co-butylene)-styrene) copolymers with 22% of saturation
SBEBBS-52	Poly (styrene-(butadiene-ethylene-co-butylene)-styrene) copolymers with 52% of saturation
SBEBBS-77	Poly (styrene-(butadiene-ethylene-co-butylene)-styrene) copolymers with 77% saturation
PMA-0	Asphalt modified by SBS
PMA-22	Asphalt modified by SBEBBS-22
PMA-52	Asphalt modified by SBEBBS-52
PMA-77	Asphalt modified by SBEBBS-77

REFERENCES

- ¹J. H. Collins and M. G. Bouldin, *Rubber World* **206**(5), 32 (1988).
- ²J. R. Fields, U.S. Patent 5,929,144, July 27, 1999.
- ³Y. Becker, M. P. Mendez, and Y. Rodriguez, *Vision Tecnol.* **9**(1), 39 (2001).
- ⁴J. S. Chen, M. C. Liao, and M. S. Shiah, *J. Mater. Civ. Eng.* **14**(3), 224 (2002).
- ⁵X. Lu and U. Isacsson, *Mater. Struct./Matériaux et Construction*. Vol. 30, preprint (1997).
- ⁶D. Lesueur and J. F. Gerard, *J. Rheol.* **42**, 1059 (1998).
- ⁷G. Wen, Y. Zhang, Y. Zhang, K. Sun, and Y. Fan, *Polym. Test.* **21**, 295 (2002).
- ⁸R. M. Ho, A. Adedeji, D. W. Giles, D. A. Hajduk, C. W. Macosko, and F. S. Bates, *J. Polym. Sci.: Part B: Polym. Phys.* **35**, 2857 (1997).
- ⁹A. Adedeji, T. Grünfelder, F. S. Bates, C. W. Macosko, *Polym. Eng. Sci.* **36**, 1707 (1996).
- ¹⁰G. Kraus, *RUBBER CHEM. TECHNOL.* **58**, 1389 (1982).
- ¹¹B. Brûlé, Y. Brion, and A. Tanguy, *Asphalt Paving Technol.* **57**, 41 (1988).
- ¹²M. G. Bouldin and J. H. Collins in "Polymer Modified Asphalt Binders," ASTM STP No. 1108, Jenneth R. Wardlaw and Scott Shuler, Eds., 1992, p. 50.
- ¹³J. F. Masson, L. Pelletier, and P. Collins, *J. Appl. Polym. Sci.* **79**, 1034 (2001).
- ¹⁴G. R. Himes (to Shell Oil Co.) U.S. RE36,757, June 27, 2000.
- ¹⁵J. G. Bardet, M. L. Gorbaty, and N. C. Nahas (to Exxon Research & Engineering Co.) U.S. 5,248,407, Sep. 28, 1993.
- ¹⁶V. A. Escobar, A. Petit, F. Pla, and R. Herrera, *Eur Polym J.* **39**, 1151 (2003).
- ¹⁷Y. Mohajer and G. L. Wilkes, *Polymer* **23**, 1523 (1982).
- ¹⁸X. Guo, P. J. Scott, G. L. Rempel, *J. Mol. Catal.* **72**, 193 (1992).
- ¹⁹G. A. Cassano, E. M. Vallés, and L. M. Quinzani, *J. Rheol.* **44**(1), 47 (2000).
- ²⁰T. S. Coolbaugh, F. C. Loveless, J. E. Marlin, D. N. Matthews, and F. P. Shirazi (to Mobil Oil Co.) U.S. 6,054,539, April 25, 2000.
- ²¹S. Bhattacharjee, P. Rajagopalan, A. K. Bhowmick, and B. N. Avasthi, *J. Appl. Polym. Sci.* **49**, 1971 (1993).
- ²²G. Cassano, E. M. Vallés, and L. M. Quinzani, *Polymer* **39**, 5573 (1998).
- ²³S. Nikhil Kumar and S. Swaminathan Sivaram, *Polym. Bull.* **35**, 121 (1995).
- ²⁴M. De Sarkar, P. De Prajna, and A. K. Bhowmick, *J. Appl. Polym. Sci.* **66**, 1151 (1997).
- ²⁵"KRATON Thermoplastic Rubber In Asphalt Products," Technical Bulletin Shell Chemical Company. USA, February 1987.
- ²⁶AASHTO-AGC-ARTBA Joint Committee. Subcommittee On New Highway Materials, Task Force 31 Report, Guide Specifications Polymer Modified Asphalt. USA, February 1992.
- ²⁷P. M. Claudy, J. M. Létouffé, D. Martin, and J. P. Planche, *Thermochim. Acta.* **324**, 203 (1998).
- ²⁸J. P. Planche, P. M. Claudy, J. M. Létouffé, and D. Martin, *Thermochim. Acta.* **324**, 223 (1998).

- ²⁹J. F. Masson and G. M. Polomark, *Thermochim. Acta.* **374**, 105 (2001).
³⁰D. Lesueur and J. F. Gerard, *J. Rheol.* **40**, 813 (1996).
³¹M. Y. Becker, A. J. Muller and Y. Rodriguez, *J. Appl. Polym. Sci.* **90**, 1772 (2003).
³²M. Marateanu and D. Anderson, *Asph. Pav. Technol.* **65**, 408 (1996).

[Received November 2004, revised April 2005]